

**DECLASSIFIED**

**BNWL-673**

BEST AVAILABLE  
REPRODUCED COPY

**DECLASSIFIED** by CG-NMP-2, 9/00 and  
Approved for Public Release  
Name/Date *Du33 Helmer 5/13/03*  
Name/Date *W.F. Nicabe 5-14-03*  
ORG: *PNNL NSAT*

*7E Savely 5-20-03-M. Shene 6/13/03*

**DECLASSIFIED**

**CONFIDENTIAL**

## C-92a. Systems for Nuclear Auxiliary Power (SNAP) - Isotopic

This document contains information that is not available for the Human Affairs Program

## 89950

Edited by K. Drumheller and R. K. Robinson  
Materials Development Section  
Materials Department

January 1968

# LEGAL NOTICE

# LEGAL NOTICE

This report was prepared as an account of Government sponsored work. Neither the United States, nor the Commission, nor any person acting on behalf of the Commission: (1) makes any warranty, or representation, expressed or implied, with respect to the use of any information, apparatus, method, or process disclosed in this report may not infringe any copyright, patent, trademark, or other rights of any person; (2) assumes any liability with respect to the use of, or for damages resulting from the use of, any information, apparatus, method, or process disclosed in this report; (3) assumes any liability with respect to the use of, or for damages resulting from the use of, any information, apparatus, method, or process disclosed in this report, to the extent that the use of any information, apparatus, method, or process disclosed in this report was not in accordance with the provisions of the Commission's policy on the use of such information, apparatus, method, or process.

As used in the above, "person acting on behalf of the Commission," includes any employee or contractor of the Commission, or employee of such contractor or contractor of such employee or contractor of the Commission, or employee of such contractor, or contractor of such employee or contractor of the Commission, or provides access to, any information with such contractor, with the Commission, or his employment with such contractor.

Document contains Restricted Data. The Atomic Energy Act of 1954. Its contents in any manner to any unauthorized person is prohibited.

PACIFIC NORTHWEST LABORATORY  
RICHLAND, WASHINGTON

**DECLASSIFIED**

**DISTRIBUTION OF THIS REPORT IS LIMITED  
To Government Personnel and Civil Contractors**

actors  
903

UNCLASSIFIED

ii

BNWL-673

Printed in the USA. Charge \$0.75.  
Available from the  
U. S. Atomic Energy Commission  
Division of Technical Information Extension  
P. O. Box 62, Oak Ridge, Tennessee  
Please direct to the same address inquiries covering the  
procurement of other classified AEC reports.

UNCLASSIFIED

TABLE OF CONTENTS

LIST OF FIGURES . . . . .	v
LIST OF TABLES . . . . .	vi
SUMMARY . . . . .	vii
POLONIUM ENCAPSULATION STUDIES . . . . .	1
Microencapsulation Principles . . . . .	1
Chemical Vapor Deposition (CVD) Studies . . . . .	5
Tellurium-Rare Earth Reaction Studies . . . . .	11
Fueling Studies . . . . .	14
Oxidation Resistant Coatings . . . . .	18
Nondestructive and Destructive Testing and Evaluation. . . . .	21
Microsphere Quality Control Techniques . . . . .	21
CURIUM OXIDE PHASE STUDIES . . . . .	25
NASA GODDARD MICROTHRUSTER TESTING . . . . .	29

LIST OF FIGURES

1	Effect of $^{210}\text{Po}$ Loading on Microsphere Clad Thickness and Power Density	3
2	Effect of Microsphere Packing Density in a Heat Source Capsule Versus Power Rating	4
3	Rare Earth Metal- $^{210}\text{Po}$ Reaction Chamber	12
4	Collimated Gamma Scanner	13
5	Electron Beam Gun Assembly	15
6	GdTe Fueled Microspheres	16
7	Vacuum Vapor Deposition Fueling System	19
8	The Effect of Heating and Cooling on the Nonstoichiometry of Curium Oxide	26
9	Postulated Phase Diagram for the Curium-Oxygen System	27
10	NASA Goddard Microthruster Disassembly Under Inert Gas in TIG Welding Hot	30

LIST OF TABLES

I	CVD Parameter Experiments Using $\text{TaCl}_5$ and $\text{WCl}_6$	7
II	Spectrochemical Analysis of Impurities in CVD Tantalum and Tungsten	8
III	Analytical Determinations of Impurities in CVD Tantalum	8
IV	Deposition Rates for Electron-Beam Evaporation Process	17
V	Coatings Which Have Been Reported to Protect Tungsten in Slow Moving Air	20
VI	Reported Recession Rates for Select Platinum Group Metals in Slow Moving Air	20
VII	Examples of the Problem of Interdiffusion	21
VIII	Analysis and Testing Techniques Being Investigated for Application in the Polonium Microencapsulation Program	22

DECLASSIFIED

vii  
BNWL-673

QUARTERLY PROGRESS REPORT  
SPACE ELECTRIC POWER PROGRAM  
SPACE NUCLEAR SYSTEMS DIVISION  
OCTOBER, NOVEMBER, DECEMBER 1967

SUMMARY

POLONIUM ENCAPSULATION STUDIES

Design optimization studies continue, and data indicates that an increase in microsphere size and polonium content could be made without a sacrifice of specific power or mechanical integrity. Experiments were conducted to investigate the parameters for chemical vapor deposition of tantalum and tungsten. Impurities in CVD coatings and incomplete removal of the fugitive magnesium core are two significant remaining problems. Rare earth reaction studies have begun with preparation of small quantities of GdTe in a multiple zone vacuum furnace. GdTe, Gd, and Ta have been successfully deposited by vacuum vapor deposition. Quality control methods are being developed for determining cladding thickness and fuel content. As yet, no suitable coating material has been found for protection of the microspheres on an individual particle basis using the present design criteria.

CURIUM OXIDE PHASE STUDIES

The thermal stability of curium oxides with respect to decomposition has been under study. Equilibrium oxygen dissociation pressures have been measured over the temperature and pressure intervals of 300 to 900 °C and 2 to 730 mm O<sub>2</sub>, respectively. Two intermediate phases of compositions CmO<sub>1.72</sub> and CmO<sub>1.82</sub> have been observed in the system. The results of the decomposition pressure measurements have been used to construct a phase diagram for the curium-oxygen system.

DECLASSIFIED

DECLASSIFIED

viii

BNWL-673

NASA GODDARD MICROTHRUSTER TESTING

The microthruster nozzle partially plugged after being pulsed 34 times during the second test period. Two hour pulses of ammonia at a flow rate of  $1 \times 10^{-4}$  lb/sec were used. The capsule had been in the test rig for 53 days under a vacuum environment. The capsule was removed from the test rig and disassembled in an inert atmosphere. Hastelloy-X degradation products were removed from the capsule and the outer gas envelope. The capsule was found to be leak tight and non-smearable. The microthruster has been reassembled and replaced in the test rig in a vacuum environment. The exact cause of the Hastelloy-X degradation is unknown. Further testing is being held in abeyance pending agreement on a new life test plan.

DECLASSIFIED



DECLASSIFIED

BNWL-673

QUARTERLY PROGRESS REPORT  
SPACE ELECTRIC POWER PROGRAM  
SPACE NUCLEAR SYSTEMS DIVISION  
OCTOBER, NOVEMBER, DECEMBER 1967

POLONIUM ENCAPSULATION STUDIES

R. K. Robinson

A process is being developed to encapsulate microgram quantities of  $^{210}\text{Po}$  into hollow, microsphere heat sources. Each microsphere heat source is to have its own helium gas plenum,  $^{210}\text{Po}$  fuel compound, compatibility cladding, structural cladding and oxidation resistant coating.

The work described in this report uses tellurium as a stand-in for  $^{210}\text{Po}$ . Polonium fueling experiments should begin during the next quarter.

MICROENCAPSULATION PRINCIPLES

J. E. Hansen

Parametric Design Criteria

A general design study is being conducted to relate heat source performance criteria and operating characteristics to the parameters in Battelle-Northwest's microsphere design concept. Overall development efforts are based on the design criteria itemized below. These criteria are directed towards development of a heat source design capability which will be suitable for SNAP 29 application and/or possible thermionic applications.

- The as-fabricated microspheres will have a power level of 30 to 40  $\text{W}/\text{cm}^3$  of microspheres.
- The heat source fuel will be a rare earth monopolonide possessing high temperature stability.
- Polonium containment will be insured as required by safety criteria. This will require a microsphere materials system which will endure environmental and thermal exposure as follows:

DECLASSIFIED

For a SNAP 29 Type Mission

- a) 135 days at 800 to 1200 °C in inert gas
- b) 1 hr at 1650 °C in an oxidizing and ablative atmosphere (arbitrarily selected temperature excursion due to mission abort or re-entry)
- c) X years at 1350 °C decreasing to ambient temperature in an oxidizing atmosphere (soil burial)

For a Thermionic Application

- a) X days at 1200 to 1800 °C in inert gas
  - b) 1 hr at 2000 °C in an oxidizing and ablative atmosphere (re-entry)
  - c) X years at 1500 °C decreasing to ambient temperature in an oxidizing atmosphere (soil burial)
- Individual microspheres will be provided with oxidation protection so as to be capable of surviving re-entry with polonium containment to end of life.

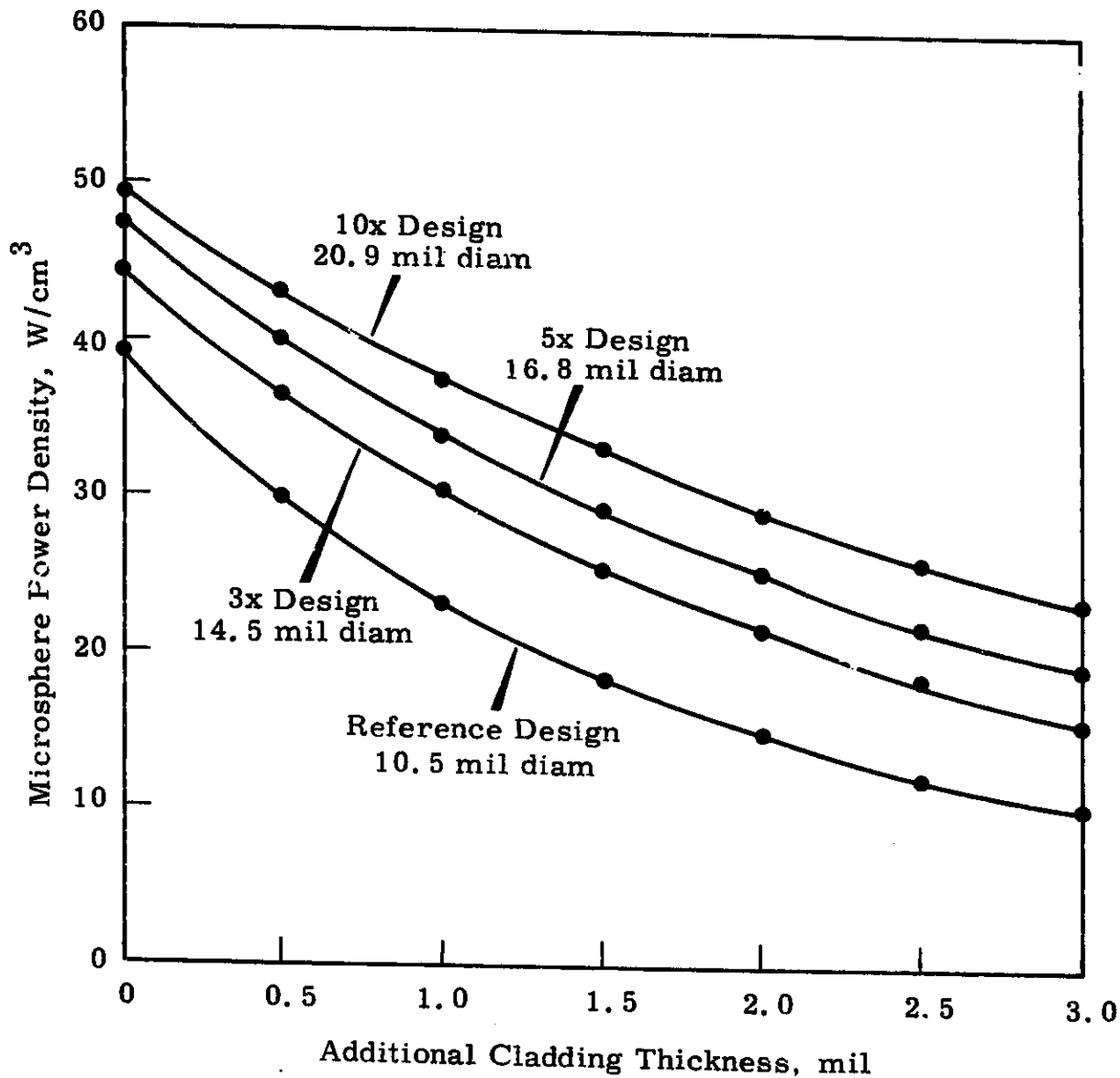
Parametric Study Status

Previous design calculations have resulted in a reference design which is mechanically capable of operating requirements. The reference design is not in optimum form. The general design study is being performed in general terms to allow for selection of a variety of microsphere designs and materials systems as a particular application requires. Plans are to adapt the design parameters to computer data processing to facilitate optimization for individual applications.

Some of the flexibility available to the microsphere concept is depicted in Figures 1 and 2. Figure 1 illustrates the potential gain in cladding thickness by increasing the polonium content and diameter of each microsphere. The notation--3x Design, 5x Design, 10x Design--refers to increasing the polonium by a factor of 3, 5, and 10, respectively, per microsphere. Since the reference design contains 2.7  $\mu\text{g}$   $^{210}\text{Po}$ , the 5x Design would contain 13.5  $\mu\text{g}$   $^{210}\text{Po}$ . The void volume is then increased so that the internal pressure and cladding stresses remain the same as in

DECLASSIFIED

Shell Thickness, Tantalum Clad (0.5 mil) Thickness, Internal Pressure, and Tungsten Clad Stress Held Constant



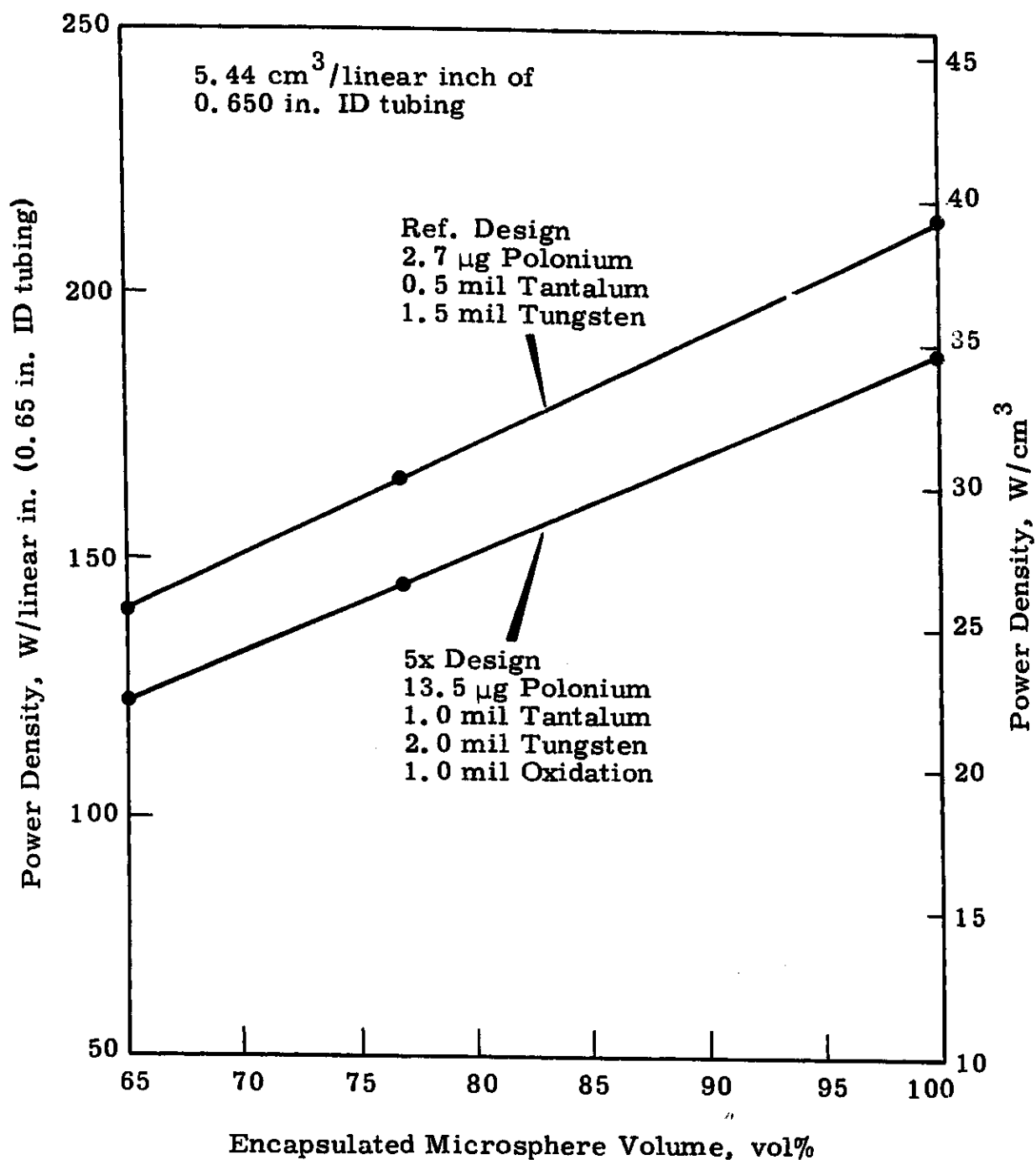
Neg 0674169-2

**FIGURE 1.** Effect of  $^{210}Po$  Loading on Microsphere Clad Thickness and Power Density

DECLASSIFIED

DECLASSIFIED

4  
BNWL-673



Neg 0674169-3

**FIGURE 2.** Effect of Microsphere Packing Density in a Heat Source Capsule Versus Power Rating

DECLASSIFIED

DECLASSIFIED

5

BNWL-673

the reference design. The net effect of increasing the fuel loading per sphere is that thicker compatibility coatings and/or oxidation coatings may be employed with no loss in specific power or mechanical integrity.

Figure 2 depicts the power rating of two microsphere designs versus sphere packing density. The 65 vol% case would be typical of a capsule containing loose microspheres, i.e., no densification. The 100 vol% case refers to the power rating of a single microsphere or a densified bed of spheres having no voids in the particle-to-particle interstices. For comparison, power density was plotted as one ordinate and linear power of a hypothetical 0.650 in. ID tube was plotted as the other ordinate.

### CHEMICAL VAPOR DEPOSITION (CVD) STUDIES

K. R. Sump

Techniques for fabricating thinwall, hollow microspheres and claddings of tantalum or tungsten are being developed and refined. The hollow microspheres are the basic building block of the microsphere heat sources. In fabricating the hollow microspheres, coatings are deposited on expendable spheres using chemical vapor deposition (CVD). After the expendable spheres are removed by vacuum vaporization and/or chemical dissolution, the rare earth element or fuel compound is deposited on the exterior of the hollow microsphere.

An alternate approach is to prepare a hollow microsphere with an internal rare earth metal cladding. This is accomplished by cladding an expendable core with a rare earth metal followed by deposition of the refractory metal and subsequent removal of the core.

#### Coating Parameters

Two CVD coating systems were used for establishing process parameters. One system was used for deposition of tungsten from  $WF_6$  using a fluidized bed of magnesium or copper microspheres. The other system was used for the establishment of the process parameters for deposition of tantalum from  $TaCl_5$  and tungsten from  $WCl_6$ . Material

DECLASSIFIED

balances were made on most of the runs in the chloride system. A balance was employed to measure the amount of coating material used in a run. A pH meter was used for monitoring the acid formation in the water scrubber solution caused by the reduction of the metal chloride by hydrogen during the run.

Several CVD parameters using the chloride coating material were investigated. The coating gas temperatures, carrier gas flow rate and the substrate material were examined with respect to coatings deposited, the reaction products generated and the reaction efficiency.

The first nine experimental runs (Table I) were made to establish a reliable process for coating a substrate with tantalum or tungsten using  $TaCl_5$  or  $WCl_6$ . The tantalum process appeared reliable but more work is required with the tungsten process. The scrubber solution was monitored with the pH meter before and after each run to check on the amount of HCl reaction product that had been formed.

Experimental runs C-10 to C-15 were made with the pH meter directly in the process line providing continuous monitoring of the hydrogen ion concentration in the scrubber solution. Each of these runs was also evaluated on the basis of the amount of  $TaCl_5$  used and the efficiency of the reduction of the halide by the hydrogen gas. The  $TaCl_5$  container was weighed before and after each run to obtain the amount of  $TaCl_5$  used. This information along with the change in hydrogen ion concentration was used to determine the efficiency of the reduction process.

### Coating Analyses

Emphasis was placed on analyzing the CVD coatings. The tantalum samples used for analysis were deposited on copper rods. Spectrochemical analysis (Table II) was made to determine metallic impurities and oxygen, fluorine and chlorine were determined analytically (Table III).

The relatively large amounts of iron, chromium and nickel in the samples were probably caused by the use of a 304 stainless steel reactor tube. The halide impurities in the tantalum are quite low. However,

DECLASSIFIED

BNWL-673

7

TAB. E.1. CVD Parameter Experiments Using  $TaCl_5$  and  $WCl_6$  (a)

Run	Coating Gas	Carrier Gas	Carrier Gas Flow Rate, cm <sup>3</sup> /min	Coating Gas Temperature, °C	Reactor Temperature, °C	Substrate	Time, hr	Amount of Coating Gas Used, g	Final pH	Efficiency %	Comments
C-1	$TaCl_5$	Ar	318	220	900	Mo rod	1				4 to 5... coating
C-2	$TaCl_5$	Ar	318	220	900	Mo rod	3				Coating gas line plugged
C-3	$TaCl_5$	Ar	113	220	900	Mo rod	2		0.79		Thick rough coating
C-4	$TaCl_5$	Ar	49	220	900	Mo rod	1		1.65		
C-5	$TaCl_5$	Ar	49	220	900	Cu tube	1				4 to 5... coating
C-6	$WCl_6$	Ar	49	240	900	Mo rod	1				Thick coat on lower end of rod and in nozzle
C-7	$WCl_6$	Ar	22	200	900	Cu spheres	1				Copper spheres stuck in nozzle
C-8	$WCl_6$	N <sub>2</sub>	49	200	900	Mo rod	1				Coating gas line plugged
C-9	$TaCl_5$	Ar	49	220	900	Mo rod	1				Good coating
C-10	$TaCl_5$	Ar	49	160	900	Mo rod	1	2.2	2.00	66	Good coating
C-11	$TaCl_5$	Ar	49	160	900	Mo rod	2	3.6	1.88	53	Good coating
C-12	$TaCl_5$	Ar	318	160	900	Mo rod	1	5.6	1.60	63	Good coating
C-13	$TaCl_5$	Ar	700	160	900	W spheres	1	4.5	2.07	29	Bad did not fluidize
C-14	$TaCl_5$	Ar	318	200	900	W spheres	1	11.7	1.30	61	4 to 5... coating
C-15	$TaCl_5$	Ar	318	180	900	W spheres	1	9.0	1.34	74	Bad did not fluidize
C-16	$TaCl_5$	Ar	318	170	900	Gd rod	2	9.58	1.78	75	Gd affected severely
C-17	$TaCl_5$	Ar	318	170	900	Cu spheres	1	4.57	1.78	52	Copper spheres stuck in nozzle
C-18	$TaCl_5$	Ar	318	170	900	Cu spheres	1	10.3	1.99	18	Leak in coating line
C-19	$TaCl_5$	Ar	318	160	900	Cu spheres	1	6.0	1.45	78	Copper spheres stuck in nozzle
C-20	$TaCl_5$	Ar	211	170	900	Cu spheres	1	4.5	1.70	64	Copper spheres stuck in nozzle
C-21	$TaCl_5$	Ar	318	170	900	Fe rod	1	1.6	2.18	55	Thin coat
C-22	$TaCl_5$	Ar	318	170	900	Fe rod	3	5.8	1.80	40	$TaCl_5$ depleted
C-23	$TaCl_5$	Ar	211	180	900	Cu rod	1	3.6	0.83	60	Thick coating
C-24	$TaCl_5$	Ar	211	180	900	GdTe rod	1	5.8	1.69	59	GdTe fractured
C-25	$TaCl_5$	Ar	211	180	900	Cu rod	2	20.0	0.96	78	Thick coating
C-26	$TaCl_5$	Ar	113	200	900	Cu rod	1	8.6	1.44	60	Thick coating
C-27	$WCl_6$	N <sub>2</sub>	12	180	550	Cu rod	1				Thin, dull coating
C-28	$WCl_6$	N <sub>2</sub>	45	180	550	SS tube	1				Thin, dull coating

(a) All runs had a  $H_2$  flow rate of 3.5 liter/min.

DECLASSIFIED

TABLE II. Spectrochemical Analysis of Impurities  
in CVD Tantalum and Tungsten

<u>Material</u>	<u>Run</u>	<u>Al</u>	<u>Be</u>	<u>Cr</u>	<u>Cu</u>	<u>Fe</u>	<u>Mg</u>	<u>Mn</u>	<u>Ni</u>	<u>Si</u>
Ta	C-23		t	m	m	s	t	m	m	m
Ta	C-25		t	m	m	s	t	m	m	t
Ta	C-26		t	s	m	s	t	m	m	t
W	C-27	s		s	s	s	m	m	s	m

TABLE III. Analytical Determinations of Impurities  
in CVD Tantalum

<u>Run</u>	<u>Fluorine</u>	<u>Chlorine</u>	<u>Oxygen</u>
C-23	< 5 ppm	33 ppm	1.9 wt%
C-25	< 5 ppm	< 10 ppm	4.5-5.0 wt%
C-26	< 5 ppm	< 10 ppm	2.4-2.9 wt%

the oxygen impurity is very high. The validity of the oxygen analysis and probable causes are being investigated.

The system for depositing tungsten from  $WCl_6$  was modified for Run C-27 and C-28. Since the  $WCl_6$  reacts with brass, an aluminum preheat cylinder was fabricated. The spectrochemical analysis (Table II) indicates that the  $WCl_6$  reacted with the aluminum as well as the stainless steel reactor. The tungsten was deposited at temperatures that would allow a magnesium substrate to be used ( $\sim 600^\circ C$ ). Metallographic analysis of the material indicates that the tungsten is oxidized. Chemical analysis is in progress. The oxygen impurity is probably due to oxygen contamination of the  $WCl_6$ .

#### CVD Coating Rare Earth Metals and Compounds

Several experiments were conducted to determine the effects of hydrogen and/or coating gases on gadolinium metal and  $GdTe$ . Run C-16 was made to determine the feasibility of directly coating gadolinium metal



by CVD.  $\text{TaCl}_5$  coating gas and hydrogen reducing gas were used. The gadolinium metal was severely affected, but the exact cause of the reaction is not known. The gadolinium appears to have hydrided with possible side effects from the vaporized halide compound.  $\text{GdTe}$  did not appear to hydride at temperatures to  $900^\circ\text{C}$  in a pure hydrogen atmosphere.

One experiment (C-24) was made to determine the feasibility of coating  $\text{GdTe}$  with tantalum by CVD. A commercially obtained  $\text{GdTe}$  rod was used for a substrate. The rod fractured into numerous pieces when heated and cooled during the coating run. Metallographic analysis revealed that the  $\text{GdTe}$  was not homogeneous. The poor quality of the  $\text{GdTe}$  prevented a good coating run and subsequent analysis.

#### Coating Equipment Design

In the earlier runs, the  $\text{WF}_6$  and  $\text{H}_2$  gases were mixed prior to entry in the reactor nozzle. The system was then modified to keep the gases separate until mixing inside the nozzle occurred. The results of this modification were that a smaller amount of  $\text{WF}_6$  was required for a specific tungsten coating thickness, the  $\text{WF}_6$ - $\text{H}_2$  reaction was more complete and the system stability was improved because tungsten coating of the nozzle orifice was greatly decreased.

Evaluation of several runs indicates that a  $\text{WF}_6$  flow rate of  $20\text{ cm}^3/\text{min}$ , a  $\text{H}_2$  flow rate of  $\sim 3000\text{ cm}^3/\text{min}$  and a reactor temperature of  $500^\circ\text{C}$  for 40 min will deposit the desired  $7.5\text{ }\mu$  thick tungsten coating on  $-100 +120$  mesh magnesium spheres.

Spectrochemical analysis of the tungsten indicates trace amounts ( $<0.01\%$ ) of Al, Cr, and Si and moderate amounts (0.01 to 1.0%) of Cu, Fe, and Mn. Analytical determinations were made on the fluorine and chlorine content of the tungsten. The fluorine impurity is quite high,  $\sim 1200\text{ ppm}$ . The chlorine is generally  $<25\text{ ppm}$ . Most of the chlorine impurity may be caused by the  $\sim 225\text{ ppn}$  chlorine impurity in the magnesium substrate material.

### Expendable Core Removal

Studies are underway to develop the best process for removal of the expendable spherical cores. During the previous program the magnesium cores were removed in the vacuum vaporization system using resistance heating and a good vacuum. Experiments using induction heating and flowing argon were performed. However, it appeared that the vacuum technique was the best, and this is being fully developed. Complete removal of all of the cores was not observed using argon. It is important that every particle core is completely removed because this directly affects the amount of void volume,  $\alpha$ , n reactions, and may also affect the compatibility of the system.

Copper and any other higher melting expendable cores will probably be removed by combination process of heating followed by chemical dissolution. If the gadolinium metal is deposited directly on the expendable core followed by a thin cladding of tungsten or tantalum, the core removal process must be entirely by vaporization since the gadolinium would be attacked by chemical dissolution. Therefore, the core material will probably be magnesium.

Removal of the expendable magnesium cores from the later tungsten clad microspheres was done with a high vacuum pumping system and an induction heater. The core removal of the first eight batches of tungsten coated magnesium spheres was limited to a maximum temperature of  $\sim 900^\circ\text{C}$ . A vacuum in the range of 0.01 to  $0.1\mu$  was obtained during the removal operation. All of the magnesium was not completely removed from the tungsten spheres. The remaining magnesium was detected by both spectrochemical and metallographic analysis. The spectrochemical analysis indicated  $>1\%$  magnesium impurity in the hollow tungsten microspheres.

The induction heating coil and vacuum containment system were redesigned so that an operating temperature of  $1500^\circ\text{C}$  was obtainable. The vacuum at temperature during core removal was 0.01 to  $0.1\mu$ .

Metallographic examination showed that all magnesium was removed. However, preliminary chemical analysis indicated a magnesium impurity level of >1%. Chemical dissolution techniques for removal of the remaining magnesium are being explored.

#### TELLURIUM-RARE EARTH REACTION STUDIES

J. E. Hansen, R. M. Fleischman, and W. J. Coleman

Rare earth metal-tellurium/polonium reactions are important to preparing suitable compound sources for direct fueling of the microspheres. An alternate approach to direct fueling by vacuum vapor deposition (VVD) is to react polonium or tellurium with microspheres containing precise amounts of active rare earth metals.

To accomplish either or both of the desired reactions, a multiple zone furnace (Figure 3) with independent zone control will be used. The reaction will take place in a vacuum tight vessel which is sealed for reaction after the atmosphere is reduced to a rough vacuum. A gamma scintillation counter (Figure 4) will monitor polonium gamma activity in the sphere zone. Reaction completeness should evidence a stabilization of gamma activity. Upon conclusion of the reaction, the excess polonium vapor will be driven to its original zone through use of a reversed temperature gradient and deposited for further use. Tellurium has been used as a polonium substrate in the initial reactions.

Reaction facilities for X Po reactions are assembled using a Lindberg 3-zone Hevi-Duty furnace with chromel-alumel thermocouples installed in each of the three zones. The three zones are controlled with Honeywell Pyr O-vane (0 to 2400 °F) controllers. Over-temperature safety is controlled with a similar controller and a second thermocouple in the center zone. A 5 cfm Welsch vacuum pump and NRC vacuum gauge are now available for evacuating the reaction vessel.

Laboratory quantities of GdTc have been prepared to provide the proper compound for vacuum vapor deposition experiments. Samples

DECLASSIFIED

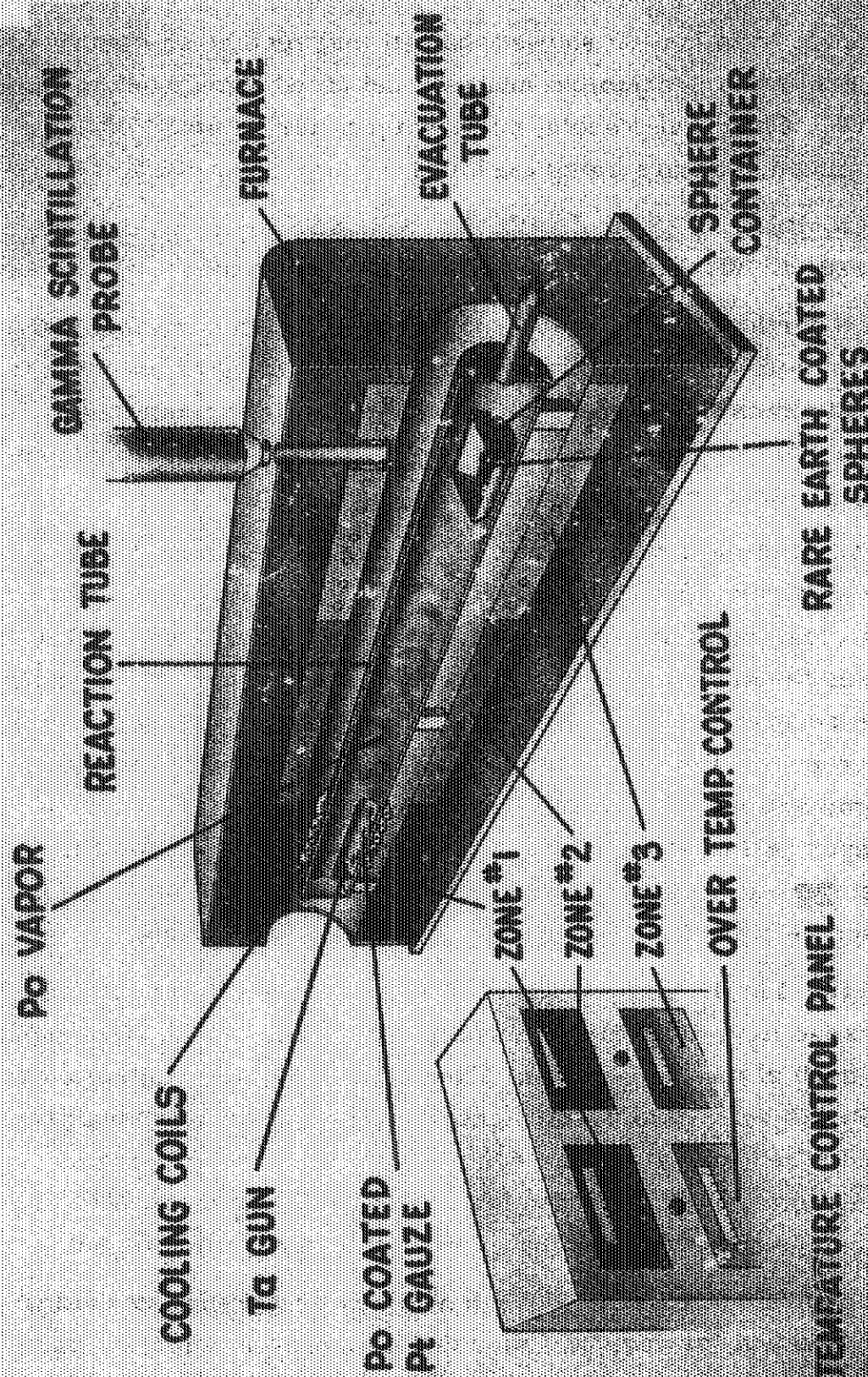


FIGURE 3. Rare Earth Metal-<sup>210</sup>Po Reaction Chamber

Neg 0674169-7

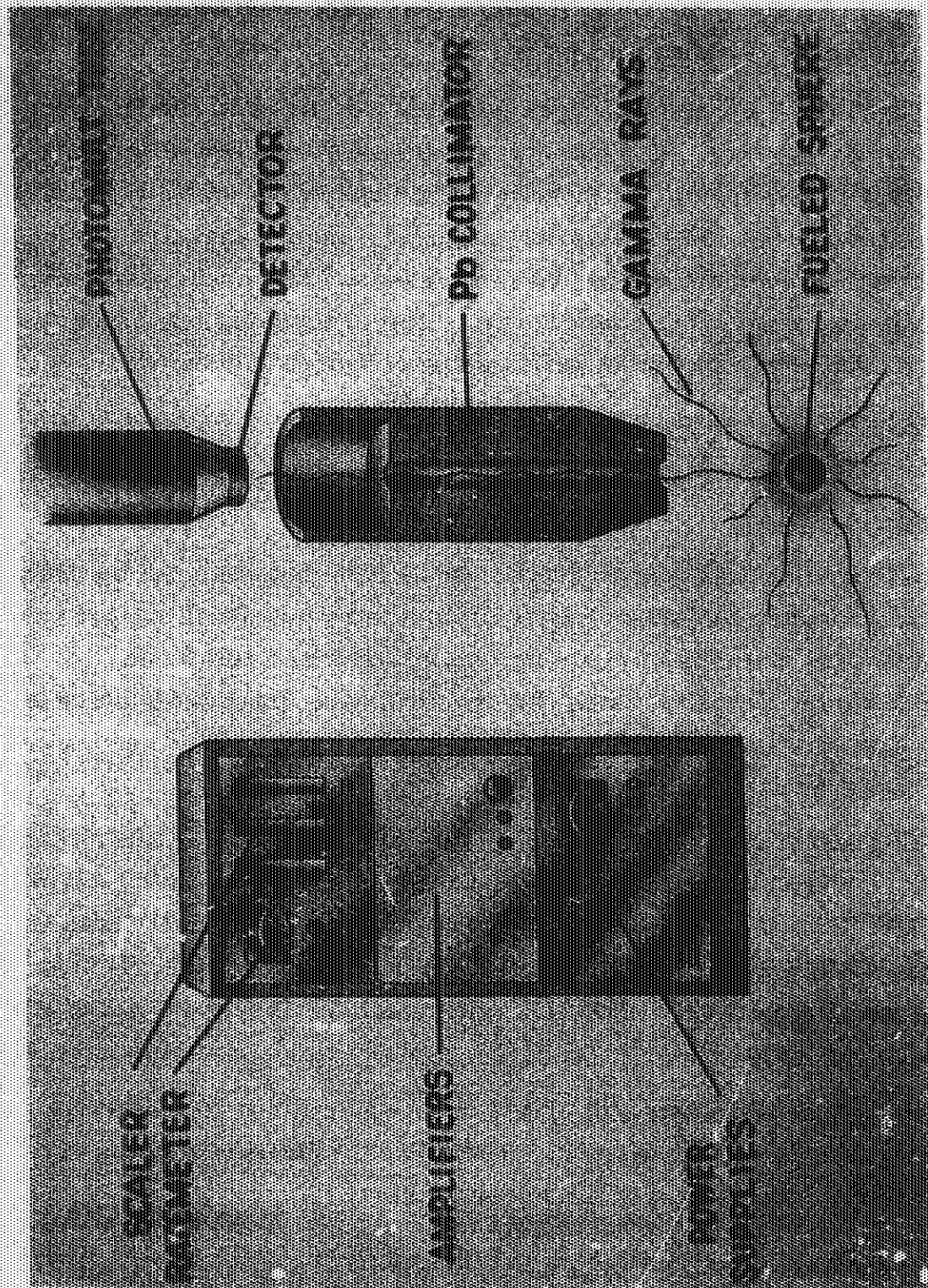
DECLASSIFIED



DECLASSIFIED

CONFIDENTIAL

13  
BNWL-673



Neg 0674159-9

FIGURE 4. Collimated Gamma Scanner

DECLASSIFIED

DECLASSIFIED

14

BNWL-673

of other candidate rare earth tellurides--DyTe, ErTe, and LuTe--are also being prepared. The GdTe preparations have been completed and are undergoing verification analyses.

A hydriding facility has been constructed and is in the final check-out stage of completion. The facility will be used to activate the rare earth metals if required prior to solid-vapor reactions of the rare earth tellurides/polonides. The activation chamber can be evacuated and back-filled with up to two inert and/or reactive gases. The processed material may be heated to 1000 °C maximum. The processing operation will take place completely within an inert gas atmosphere glovebox.

### FUELING STUDIES

W. J. Coleman and R. M. Fleischman

#### Gadolinium Telluride

Efforts to vacuum vapor deposit GdTe have been slowed by receipt of material procured as GdTe of 1:1 stoichiometry but which in fact contained significant amounts of elemental gadolinium and tellurium. Analyses of vapor deposits using this material are invalidated since it cannot be determined whether the GdTe compound present in the source material disassociated during deposition.

The present method of analyzing for GdTe is to 1) determine the gadolinium-to-tellurium ratio by X-ray fluorescence, 2) heat the sample to 700 to 800 °C in a vacuum to drive off any free tellurium, 3) determine the new gadolinium-to-tellurium ratio by X-ray fluorescence, 4) heat remaining sample to 1400 to 1500 °C to drive off any free gadolinium and 5) determine the gadolinium-to-tellurium ratio in the remaining sample.

Due to lack of a standard, the present gadolinium-to-tellurium ratio is only a relative comparison. A standard is presently being prepared which will help interpret the present data.

GdTe was deposited using downward electron-beam evaporation method (see Figure 5) and then analyzed as described above. The results indicated that deposited material was tellurium rich compared

DECLASSIFIED

DECLASSIFIED

15  
BNWL-673

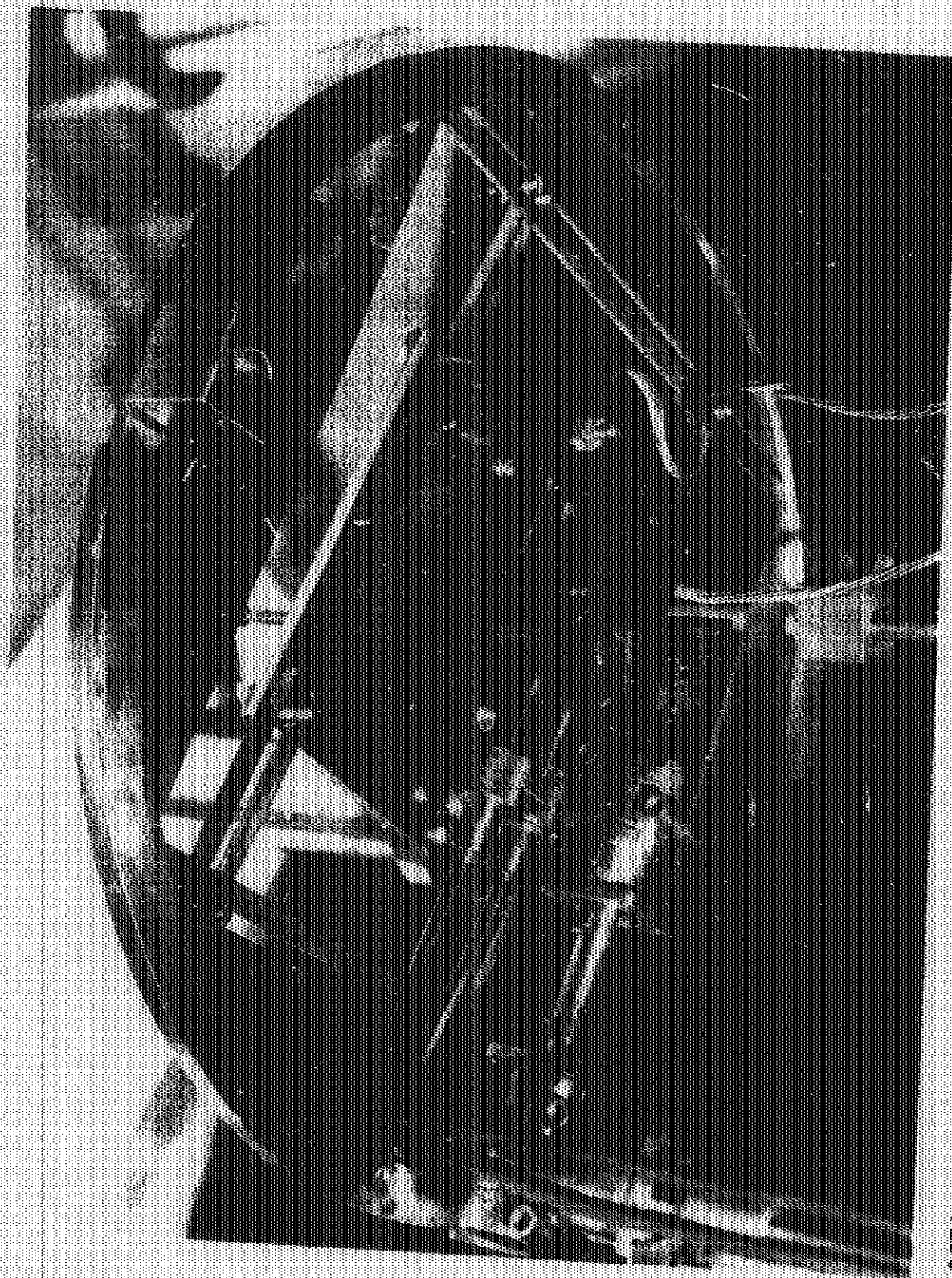


FIGURE 5. Electron Beam Gun Assembly

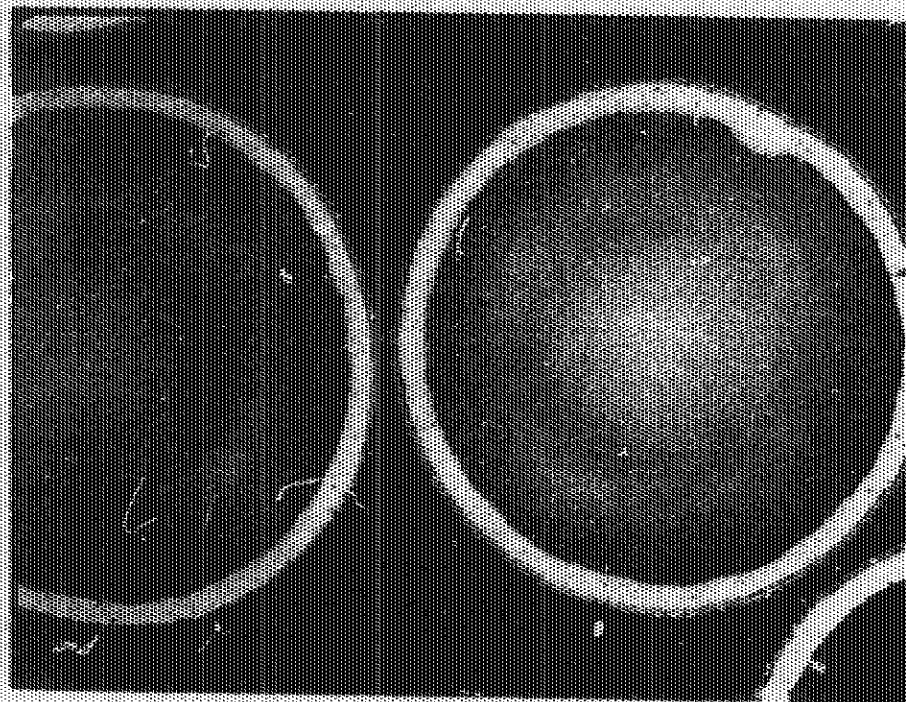
Neg 0674135-2

DECLASSIFIED



to the initial GdTe rod, also that free tellurium was deposited. With these results, the GdTe rod was checked before and after heating to 700 °C in vacuum. The results indicated that the rods have free tellurium. New GdTe is being prepared, and deposition of GdTe will be evaluated using only the compound GdTe.

Two fueling runs using the poor quality GdTe rods were made. These runs allowed an evaluation of material adherence to the spheres, evaporation rates, and thickness monitoring techniques. The adherence was acceptable and no peeling was observed on the spheres. The evaporation rate was 100 Å/sec maximum with 75 Å/sec for ideal operation. Figure 6 shows the section of some of the coated spheres. The microspheres are tungsten.



400X

FIGURE 6. GdTe Fueled Microspheres



Gadolinium Coatings

Downward evaporation of gadolinium has been achieved. Several samples have been coated using this method. The film adherence is fair, not quite as good as GdTe, but it appears to be acceptable. The evaporation rate is excellent with a maximum rate of 700 Å/sec and 500 Å/sec for normal operative conditions (See Table IV for a rate comparison of tantalum, gadolinium, and GdTe.)

TABLE IV. Deposition Rates for Electron-Beam Evaporation Process

<u>Material</u>	<u>Maximum Rate,</u> <u>Å/sec</u>	<u>Normal Rate,</u> <u>Å/sec</u>
Cd	700	500
GdTe	100	75
Ta	30	30

The same E-gun (electron-beam gun), Figure 5, has been used to do all the downward evaporation. Gadolinium coated samples are presently being prepared to use in the reaction studies. Efforts are being made to determine if an active film of gadolinium can be deposited, which would eliminate the hydride process required to activate air exposed gadolinium. A few runs have been made coating tungsten, tantalum, copper, and magnesium spheres.

Tantalum Coating

Downward evaporation of tantalum has been achieved. The film adherence is good on tungsten, fair on quartz, and poor on tantalum. The reasons for these differences have not yet been determined. The evaporation rate is slow with a maximum rate of 30 Å/sec. This appears to be due to the limited power of the E-gun supply (3 kW). The high melting temperature of tantalum probably results in a large heat loss leaving only a small percent of the original input power to be used

in evaporating the tantalum. The GdTe coated spheres were coated with a thin (approximately  $0.15\mu$  thick) tantalum film.

#### Vacuum Vapor Deposition System

The fueling system is illustrated in Figure 7. The system can be broken down into separate units: 1) vacuum system, 2) E-gun, 3) sputtering unit, and 4) particle vibrator.

The vacuum chamber is designed such that resistance heating, E-gun heating and sputtering deposits can be done jointly or separately. Initially, the sputtering unit will be installed in a bell jar system for evaluation and to establish deposition parameters. The E-gun is presently in operation.

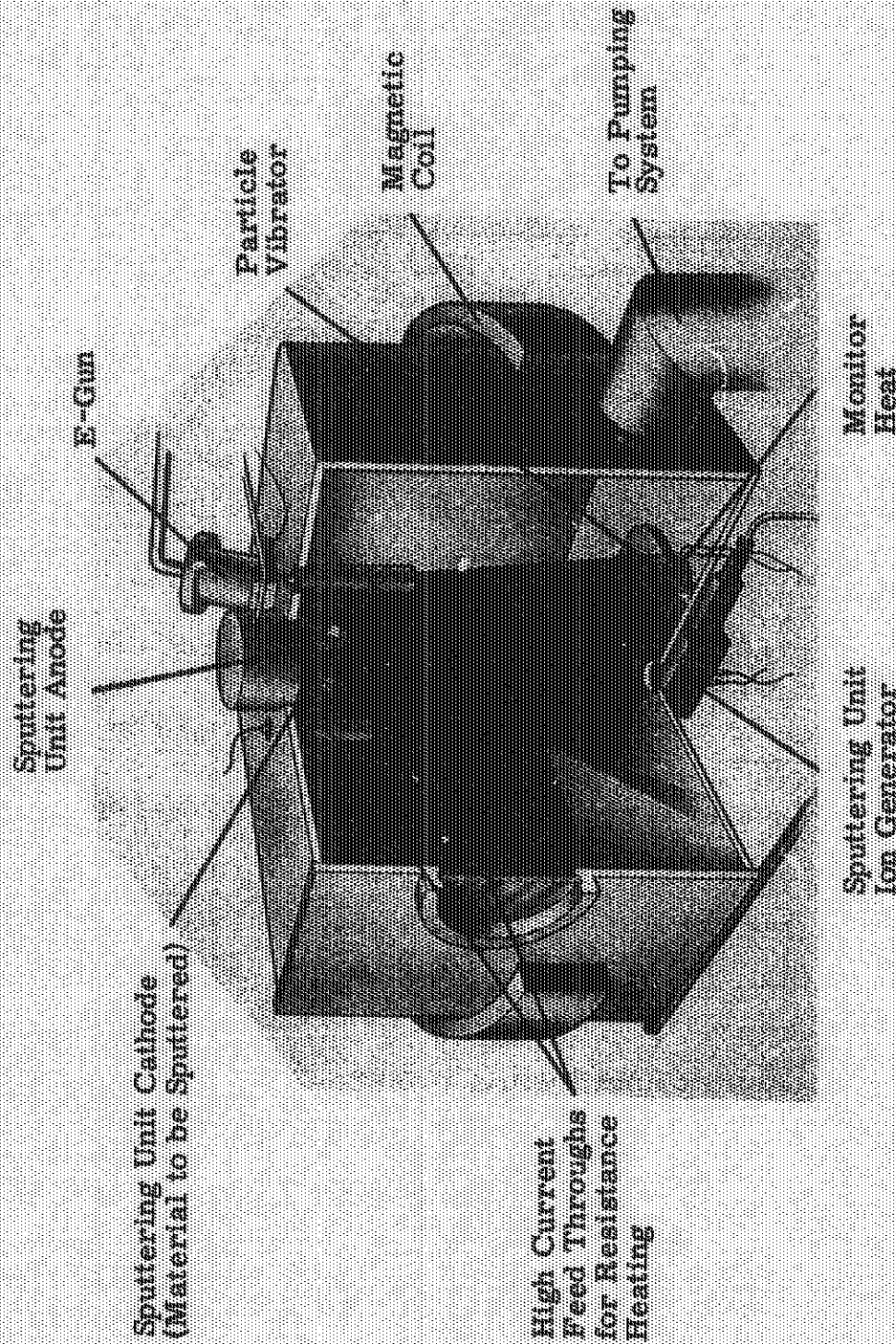
A number of devices have been tested for optimum sphere movement in the VVD coating process. Through process of elimination, low frequency ultrasonic transducers have been selected as the driving force. Four transducers are side mounted on an aluminum block. To eliminate standing wave problems, a switching mechanism between the power supply and transducers will be used to switch power among the transducers.

#### OXIDATION RESISTANT COATINGS

J. E. Hansen

Individual microspheres will possess an oxidation resistant coating to provide assurance of polonium containment in the events of individual microsphere re-entry or soil burial. The present microsphere design employs tungsten as a strength cladding. Tungsten incurs catastrophic oxidation at temperatures well below the expected operating temperatures. The oxidation resistant coating selected must protect tungsten from oxidation, and it must be as thin as possible to avoid unnecessary reduction of microsphere power density.

DECLASSIFIED



Neg 0674169-8

FIGURE 7. Vacuum Vapor Deposition Fueling System

DECLASSIFIED

A literature survey has revealed that several coating systems are available which will protect tungsten from oxidation for the required time. Examples of this information are given in Tables V and VI.

**TABLE V.** Coatings Which Have Been Reported to Protect Tungsten in Slow Moving Air

<u>Coating</u>	<u>Temperature, °C</u>	<u>Hours</u>
Silicides	1650	<10
	1300-1400	10-100
	1100	>1000
Aluminides	1900	2
Complex Oxide	1850	5
Cermet	1100	>1
Platinum Group	2000	2-5

**TABLE VI.** Reported Recession Rates for Select Platinum Group Metals in Slow Moving Air

<u>Metal</u>	<u>1200 °C</u>	<u>1500 °C</u>	<u>2000 °C</u>
	<u>Recession Rate, mils/hr</u>		
Iridium (Ir)	$1 \times 10^{-2}$	$2 \times 10^{-2}$	$10 \times 10^{-2}$
Palladium (Pd)	$1 \times 10^{-2}$	$2 \times 10^{-3}$	$10 \times 10^{-3}$
Platinum (Pt)		$1 \times 10^{-4}$	$15 \times 10^{-4}$
Rhodium (Rh)		$15 \times 10^{-5}$	$10 \times 10^{-3}$

Selection of an oxidation coating is complicated by compatibility considerations. At high operating temperatures (above 1500 °C), nearly all the tungsten coatings exhibit rapid interdiffusion with the tungsten. This means that the protective coating completely interdiffuses with the tungsten to expose a surface which is prone to oxidation. The problem of interdiffusion is illustrated in Table VII.

TABLE VII. Examples of the Problem of Interdiffusion

<u>Coating Substrate</u>	<u>Temperature, °C</u>	<u>Hours</u>	<u>Interdiffusion Distance, mils</u>
Ir-W	2025	100	2
		1000	12
		5000	16
Rh-W	1800	3	1
		1	2

The problem of interdiffusion also exists at all other materials interfaces in the microsphere design. Selection of a final oxidation resistant coating will be made after compatibility problems throughout the complete materials system have been considered and the final strength cladding material is chosen. In the interests of time, potential oxidation coatings and diffusion barrier systems will be screened concurrently with consideration of the basic materials system.

#### NONDESTRUCTIVE AND DESTRUCTIVE TESTING AND EVALUATION

J. E. Hansen

Table VIII illustrates the techniques which are being evaluated for application to the polonium microsphere fabrication process. The inherent radiation and contamination problems of handling polonium limit the utilization of several analytical facilities. However, the necessary analytical capabilities are being established and are expected to be available as required after polonium arrives on site.

#### MICROSPHERE QUALITY CONTROL TECHNIQUES

F. V. Richard and D. R. Green

Use of infrared techniques to determine quantity of polonium in completed microspheres appears plausible, provided previous (infrared or other) tests have ascertained the uniformity of cladding thicknesses. A controlled thermal environment is required in order that the emitted

TABLE VIII. Analysis and Testing Techniques Being Investigated for Application in the Polonium Micoencapsulation Program

<u>TECHNIQUE</u>	<u>POTENTIAL APPLICATION(S)</u>
1. AIR CLASSIFICATION	DIAMETER SIZING
2. ANALYTICAL CHEMISTRY	PURITY ANALYSIS OF INPUT MATERIALS, VERIFICATION OF CORE REMOVAL, STOICHIOMETRY, IDENTIFICATION OF COATING INTERFACE COMPOUNDS.
3. EDDY CURRENT	COATING THICKNESS AND UNIFORMITY, COATING BONDING.
4. GAMMA SCANNER	QUANTITY VERIFICATION OF RARE EARTH POLONIDE DEPOSIT.
5. HELIUM LEAK TEST	VERIFICATION OF POLONIUM CONTAINMENT.
6. INCLINED VIBRATION	PARTICLE SPHERICITY INSPECTION.
7. INFRA-RED	QUANTITY VERIFICATION OF RARE EARTH POLONIDE DEPOSIT, COATING THICKNESS UNIFORMITY.
8. METALLOGRAPHY	PRODUCT INTEGRITY AT EACH PROCESS STEP, DIMENSIONAL INSPECTION.
9. MICROCALORIMETRY	QUANTITY VERIFICATION OF RARE EARTH POLONIDE DEPOSIT, QUALIFICATION TESTING.
10. MICROPROBE	PRODUCT INTEGRITY, COATING INTERFACE ANALYSIS.
11. MICROSCOPIC	DIMENSIONAL INSPECTION.
12. MICRORADIOGRAPHY	PRODUCT INTEGRITY, COATING BOND INSPECTION, QUALIFICATION.
13. MONITOR SLIDES	IN-PROCESS COATING DEPOSIT THICKNESS CHECK.
14. PARTIAL PRESSURE	THERMAL QUALIFICATION TEST
15. PROPERTIES ANALYSES	MECHANICAL PROPERTIES, QUALIFICATION.
16. RINSE TEST	VERIFICATION OF POLONIUM CONTAINMENT.
17. SCREENING	DIAMETER SIZING, SORTING.
18. WEIGHT GAIN	QUANTITY TUNGSTEN DEPOSIT CHECK.

DECLASSIFIED

DECLASSIFIED

DECLASSIFIED

23

BNWL-673

infrared be an unambiguous function of quantity of fuel. Preliminary ideas include: 1) support of individual spheres in a thin constant temperature jet of gas with subsequent determination of infrared emission, 2) immersion of several spheres in a fluid heat sink with a thin Mylar bottom allowing infrared scanning to determine sphere temperatures, 3) a similar heat sink with the Mylar replaced by a thin phosphor coated plate which when excited by ultraviolet will emit visible light in accordance with sphere temperature, and 4) infrared measurements on free falling spheres. Experiments to determine feasibility and ease of manipulation of spheres will be necessary.

Some computer work has been initiated to calculate surface temperature as a function of quantity of fuel and as a function of non-uniform cladding thicknesses presuming uniform fuel distribution. The latter calculations were designed to determine feasibility of using infrared to check for nonuniform cladding thicknesses. Once a testing environment is chosen, calculations of surface temperature as a function of fuel content can be utilized to determine the expected infrared emission.

Methods for determining cladding thicknesses are still being investigated. Preliminary results of X-ray microscopy work indicate that, with additional development, the void diameter and total wall thickness can be observed for a particular plane of observation through the microsphere. Although difficulty was anticipated in distinguishing between the various layers, subsequent experimentation with longer exposure times and lower tube voltages has revealed some structure in the wall, possibly the polonium layer. Further investigation seems warranted. A pulsed resonant ultrasonic technique for determining cladding thicknesses has been looked into but does not appear promising at present.

Further work will probably be concentrated in the areas of X-ray microscopy, X-ray fluorescence, infrared techniques, and electromagnetic methods.

DECLASSIFIED

CURIUM OXIDE PHASE STUDIES

T. D. Chikalla

The thermal stability of curium oxides with respect to decomposition has been under study. Equilibrium oxygen dissociation pressures have been measured over the temperature and pressure intervals of 300 to 900 °C and 2 to 730 mm O<sub>2</sub>, respectively. All of the isobaric temperature-composition plots showed broad hysteresis loops remarkably similar to those observed in tensimetric studies on the praseodymium-oxygen system. The nonstoichiometric compositions encountered in the p-T interval examined extend over  $1.6 < (O/Cm) < 2$ . Two intermediate phases have been observed in the system; and, based on the assumption that curium is completely tetravalent at 300 °C in 1 atm O<sub>2</sub>, the calculated compositions of these phases are CmO<sub>1.72</sub> and CmO<sub>1.82</sub>. These phases have been designated  $\iota$  and  $\delta$ , respectively, while nonstoichiometric phases occurring near the dioxide and sesquioxide composition have been termed  $\alpha$  and  $\sigma$ .

In one series of runs at 159 mm O<sub>2</sub>, the effects of heating and cooling rates were studied by traversing the interval 300-900-300 °C in total times of 24, 72, and 144 hr. The results from the 24 and 72 hr runs are shown in Figure 8. At the slower heating rate, the system breaks into the ( $\alpha + \delta$ ) region at a lower temperature; and, except for a sharper  $\delta$  break, the isobar parallels that obtained over the 24 hr cycle to the  $\iota$  region where the isobars are coincident. The break out of the  $\iota$  phase occurs at a slightly higher temperature for the lower heating rate, and in fact, the entire hysteresis loop during both heating and cooling is shifted toward slightly higher compositional (or temperature) values. On cooling through  $\iota$ , the curves at these two heating rates are again nearly coincident. The results from the 144 hr run were complicated by a slight zero shift in the balance. If the appropriate correction is applied to these data, the curve during both heating and cooling nearly coincides with that obtained during the 72 hr cycle. These results indicate that the hysteresis



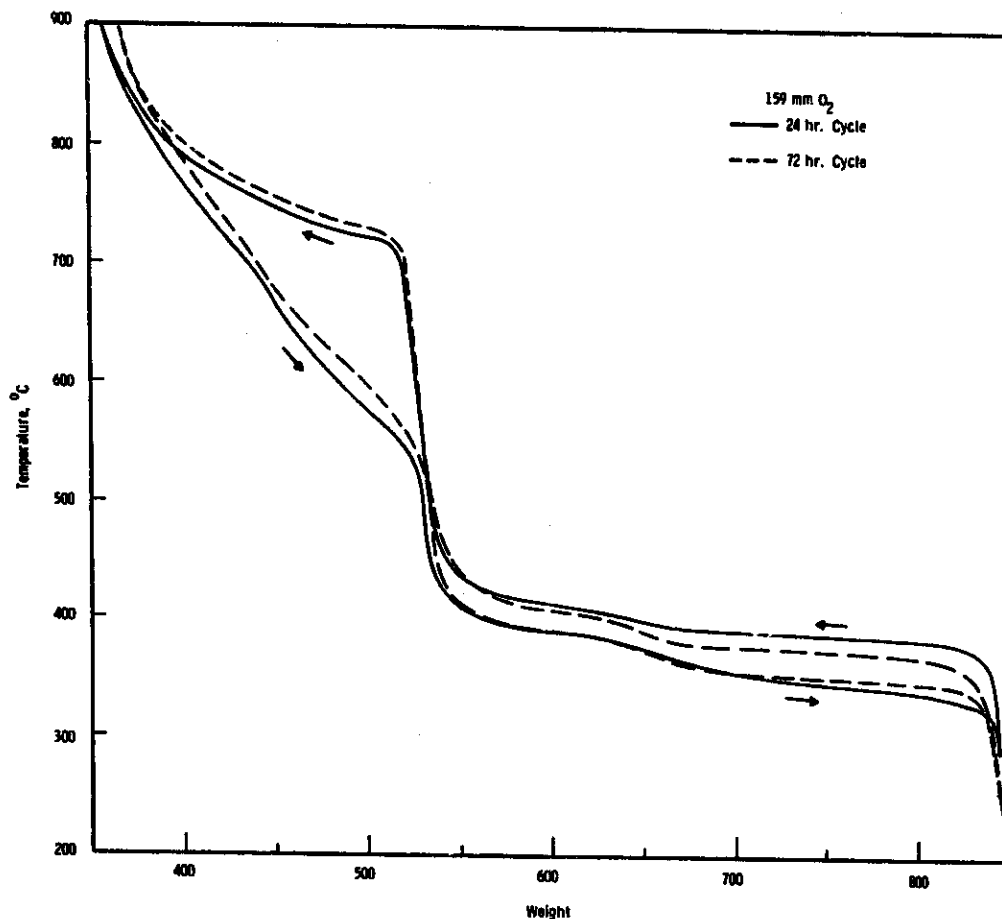


**FIGURE 8.** The Effect of Heating and Cooling on the Nonstoichiometry of Curium Oxide. A 72 hr cycle results in a slight closure of the hysteresis loops.

loop in the  $(1 + \sigma)$  region is not significantly altered when the heating and cooling rates are changed by a factor of six although the  $(1 + \delta)$  loops are reduced in size. This is similar to the results on the lanthanide system and no doubt is influenced by the low temperature of the  $(1 \pm \delta)$  reaction.

The results of the decomposition pressure measurements have been used to construct, to a first approximation, a phase diagram for the

curium-oxygen system. The diagram is shown in Figure 9, where the compositions and temperatures of the various phase transformations have been taken from the original weight-temperature versus time records. All of the dashed lines are highly uncertain and are included simply to suggest an analogy to the rare earth oxides. The peritectoidal decomposition temperatures of 1000 °C for  $\gamma$  and 500 °C for the  $\delta$  phase are chosen on the basis of corresponding temperatures in lanthanide oxide systems. The compositional width of the single phase regions have also been arbitrarily chosen. The apparently wide  $\gamma$  region shown is probably due to impurities in the sample (principally americium) while the  $\delta$  phase width is due to a sluggishness resulting from low temperatures, and both may be influenced by the structural damage caused by the intense radioactivity.

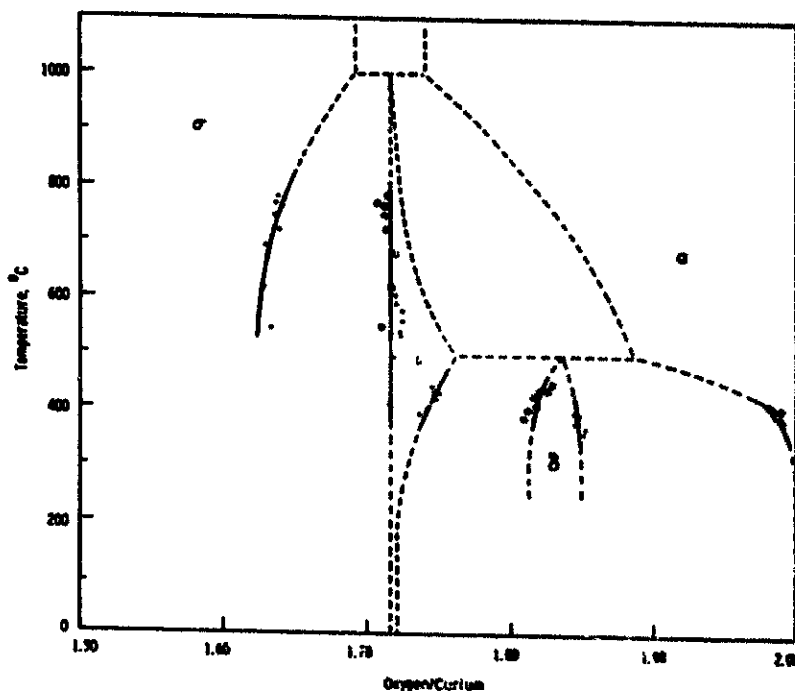


**FIGURE 9.** Postulated Phase Diagram for the Curium-Oxygen System. Open and closed circles represent transformations observed on heating and cooling, respectively. Location of dashed lines is approximate.

DECLASSIFIED

28

BNWL-673

There is insufficient data to determine whether or not the  $\delta$  phase actually decomposes eutectoidally at low temperatures and low pressures as indicated in the low pressure runs and as has been suggested in the Pr-O system. Indeed, a plot of  $RT \ln pO_2$  versus T for the various transformations shows the ( $\alpha - \delta$ ) boundary crossing the ( $\delta - \epsilon$ ) boundary at a temperature on the order of 330°C, suggesting a ( $\delta \rightarrow \epsilon + \alpha$ ) decomposition. However, the slope of these plots is extremely susceptible to errors in pressure, especially at low  $pO_2$ , and great significance is not attached to this fact. Efforts to investigate this occurrence experimentally were hampered by kinetic effects at the low temperatures involved.

DECLASSIFIED

NASA GODDARD MICROTHRUSTER TESTING

V. L. Hammond and B. Norton

The microthruster was inspected in early August 1967 and installed in the test rig on August 23, 1967 for the second series of ammonia flow tests.

The microthruster nozzle partially plugged after being pulsed 34 times during the second test period with 2-hr pulses of ammonia at a flow rate of  $1 \times 10^{-4}$  lb/sec. The thruster had been in the test rig for 53 days under a vacuum environment except when being pulsed with ammonia. The plugging of the nozzle was detected by the rise in the thruster chamber during the ammonia tests. The chamber pressure at the end of the first ammonia pulse was 21 psia and, by October 27, 1967, had increased to 29 psia at the end of the 33rd pulse. This increase was continuous to this time.

The inlet orifice pressure was 85 psia for all pulses. The next and last ammonia flow test was made on October 30, 1967; the chamber pressure at the end of this test was 34 psia. All pressure instrumentation was calibrated and it was determined that the nozzle had become partially plugged.

After all concerned parties were notified and agreement was reached on the course of action, the thruster was removed from the test rig on November 3, 1967 and transported to 324 Building in the shipping cask for disassembly. The disassembly, inspection, and degradation product removal was started on November 6, 1967 and was continued through November 8, 1967. NASA Goddard Space Flight Center and General Electric Company Personnel were on hand to watch the disassembly and inspection.

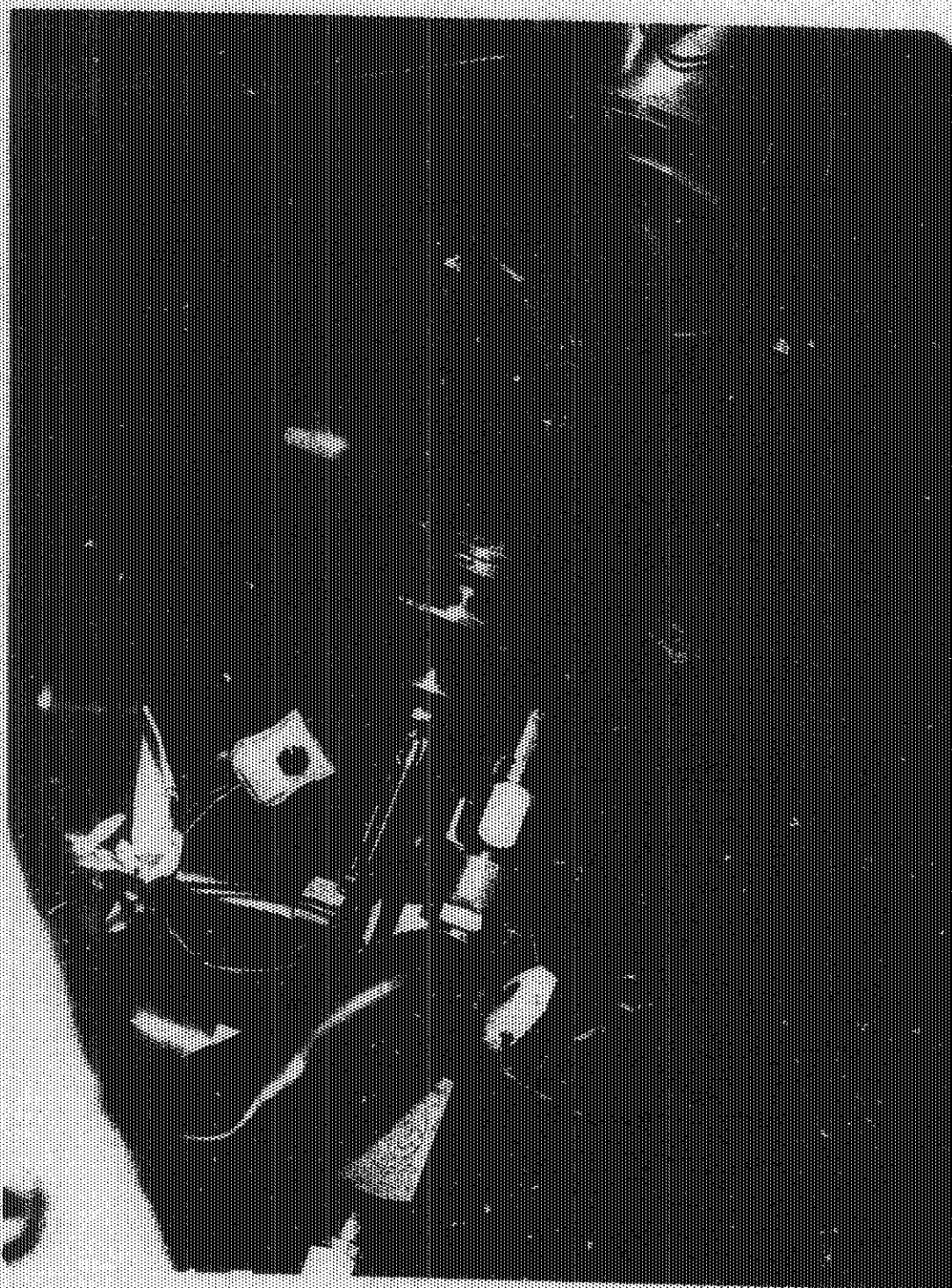
The assembly was transferred into a welding hood and disassembled under an argon atmosphere (see Figure 10). The degradation products were

DECLASSIFIED

~~CONFIDENTIAL~~

30

BNWL-673



Neg 0673793-1

**FIGURE 10.** NASA Goddard Microthruster Disassembly Under Inert Gas in TIG Welding Hood

~~CONFIDENTIAL~~

DECLASSIFIED

removed from the capsule and placed in an air-tight container under an argon atmosphere in the welding hood. The heat shield assembly and  $^{147}\text{Pm}$  capsule were allowed to cool overnight in the welding hood before they were placed in open air. The degradation products were removed from the outer gas envelope of the heat shield package in air. The degradation products on the capsule varied from a dark gray to a greenish-gray in color and the surface had a matted appearance. Photographs were taken of each step in the disassembly to provide complete documentation.

The following analyses and measurements were made on the degradation products and microthruster components:

<u>Analyses and Measurements</u>	<u>Results</u>
1. Degradation Products	
Emission Spec. Analysis	Hastelloy-X Powder
X-ray Diffraction Analysis	Fe-Ni Alloy and $\text{Cr}_2\text{O}_3$
Gas Fusion Analysis (% weight)	1% $\text{N}_2$ , 20% $\text{O}_2$
Carbon Analysis	180 ppm
2. Thruster Components	
Capsule Ultrasonic Wall	
Thickness Measurement	0.0180 to 0.0216 in. wall thickness
Capsule OD Measurement at 225 °F	1.1855 to 1.1895 in.
Estimated External Wall Thickness Loss	0 to 0.0015 in.
Estimated Internal Wall Thickness Loss	0.0019 to 0.0055 in.

No leaks could be detected in the heat source by leak checking with a helium mass spectrometer or by smearing the capsule and checking for radiation contamination. After the degradation products were removed from all the thruster components, it was reassembled and returned to 324 Building for insertion into the test rig.

The rear heat shield was removed and repaired during the inspection. A new thermocouple was fabricated and installed in the core. The thermocouple seats in the bottom of the thermocouple well and is

DECLASSIFIED

32

BNWL-673

spring loaded. The thermocouple well was cleaned to insure metal to metal contact. The thruster has been held in a vacuum since the first of December 1967. The vacuum increased from  $5 \times 10^{-5}$  Torr at the first of December to  $5 \times 10^{-6}$  Torr by the end of December. The thermocouple was indicating a capsule skin temperature of 1250 °F the first of December which is approximately what the original thermocouple is estimated to have indicated at that date.

The thruster will be held in the test rig under a vacuum environment until all concerned parties have reviewed the analyses of the degradation products and agree on a new life test plan. The exact cause of the Hastelloy-X degradation has not been established at this time and may require an extensive compatibility testing program to evaluate and determine the degradation process that is taking place. No further ammonia flow tests are planned at this time.

DECLASSIFIED